Effect of inorganic and organic ligands on the sorption/desorption of arsenate on/from Al–Mg and Fe–Mg layered double hydroxides

A.G. Caporale [a], M. Pigna [a], J.J. Dynes [b], V. Cozzolino [a], J. Zhu [a], A. Violante [a,*]

[a] Department of Soil, Plant, Environment and Animal Production Science, Faculty of Agriculture, Via Università 100, 80055 Portici (Napoli), University of Naples Federico II, Naples, Italy
[b] Canadian Light Source, University of Saskatchewan, 101 Perimeter Road, Saskatoon, SK S7N 0X4, Canada

ABSTRACT

This paper describes the sorption of arsenate on Al–Mg and Fe–Mg layered double hydroxides as affected by pH and varying concentrations of inorganic and organic ligands, and the effect of residence time on the desorption of arsenate by ligands. The capacity of ligands to inhibit the fixation of arsenate followed the sequence: nitrate < nitrite < sulphate < selenite < tartrate < oxalate ≪ phosphate on Al–Mg-LDH and nitrate < sulphate ≈ nitrite < tartrate < oxalate < selenite ≪ phosphate on Fe–Mg-LDH. The inhibition of arsenate sorption increased by increasing the initial ligand concentration and was greater on Al–Mg-LDH than on Fe–Mg-LDH. The longer the arsenate residence time on the LDH surfaces the less effective the competing ligands were in desorbing arsenate from sorbents. A greater percentage of arsenate was removed by phosphate from Al–Mg-LDH than from Fe–Mg-LDH, due to the higher affinity of arsenate for iron than aluminum.

© 2011 Elsevier B.V. All rights reserved.

1. Introduction

In recent decades, a class of anionic clays known as layered double hydroxides (LDHs) have attracted substantial attention due to their potential use in many applications, such as photochemistry, electrochemistry, polymerization, magnetization, biomedical science and environmental clean-up [1–7]. For example, LDHs could be used in pharmaceutical formulations and for new drug delivery systems in biomedical science [4,5]. There has also been considerable interest in using LDHs as adsorbents to remove environmental contaminants due to their large surface area, high anion exchange capacity (2–3 mequiv. g^{-1}), and good thermal stability [1,6]. In addition, LDHs are also relatively simple and economical to synthesize by coprecipitation methods under laboratory conditions [1,7], thus they can be produced in large quantities. LDHs also form in soil environments and present peculiar sorption capacities [8].

LDHs can be represented by the general formula $[M^{2+}_{1-x} M^{3+}_x (OH)_6]^{x+} [(A^{n-})_{x/n} m H_2O]^{x-}$, where x is the molar ratio $M^{3+}/(M^{2+} + M^{3+})$, taking values between 0.20 and 0.33, while M^{2+} and M^{3+} are divalent (Ca, Mg, Co, Fe, Cu, Ni, Mn) and trivalent metal cations (Al, Fe, Cr), respectively, and A is an interlayer anion (e.g., Cl, NO_3, ClO_4, CO_3, SO_4) of valence n. They are composed of positively charged brucite-like sheets and the positive charges are balanced by intercalation of anions in the hydrated interlayer regions, analogous to the cationic clays whose negative charge of the aluminosilicate layers are counterbalanced by cations [1,7,9–11]. The LDHs have relatively weak interlayer bonding and, as a consequence, the original anions sorbed in the interlayer are easily exchanged with many inorganic and organic anions by simple ion exchange methods.

Arsenic (As) concentrations in drinking waters in excess of 1.33×10^{-7} mol L^{-1} (0.01 mg As L^{-1}) are considered to be hazardous to the welfare of humans and animals [12–16]. However, the As concentration of drinking water for millions of people exceeds 1.33×10^{-7} mol L^{-1}, with tens of thousands already suffering from skin, lung and liver cancer, and melanosis. Natural sources, such as the dissolution of As containing bedrock, often contribute significantly to the As content of drinking water and groundwater. Despite environmental restrictions and regulations limiting the production and uses of As, significant amounts are still introduced into water through the dissolution of minerals and ores, from industrial effluents, via atmospheric deposition, from agriculture, forestry chemicals and fertilizers [13,14].

As exists predominantly as the trivalent (+3) and pentavalent (+5) states in aqueous solution. Generally, arsenite (AsO_3) species are more toxic than arsenate (AsO_4) ones. The distribution of AsO_4 species in natural waters is mainly dependent on the redox potential and pH [13,14]. Most As removal technologies from contaminated water treat AsO_4 much more effectively than AsO_3, so a pre-oxidation step is recommended for source waters containing AsO_3 at significant concentrations [14].

* Corresponding author. Tel.: +39 081 2539175; fax: +39 081 2539186.
E-mail address: violante@unina.it (A. Violante).

Fe and Al oxides have been widely studied as sorbents for controlling the concentration of As in natural waters [13–18]. LDHs have shown great potential to efficiently remove As from aqueous systems [11,16,19–21]. The effect of competing anions on AsO_4 sorption/desorption on/from Al or Fe oxides has been extensively studied [8,15,22–25], while only a few studies have examined the effect of competing anions (e.g., phosphate, carbonate, sulphate, fluoride, chloride, bromide, nitrate) on the efficiency of LDHs to remove As from aqueous systems [26,27].

In the present work, the competition between AsO_4 with organic and inorganic ligands for the sorption sites on two LDHs, obtained by coprecipitating Mg with Al (Al–Mg-LDH) or Fe (Fe–Mg-LDH), was studied. Specifically, we examined (i) AsO_4 sorption on Al–Mg-LDH and Fe–Mg-LDH as affected by pH and varying concentrations of inorganic [nitrate (NO_3), nitrite (NO_2), phosphate (PO_4), selenite (SeO_3), sulphate (SO_4)] and organic [oxalate (OX), tartrate (TAR)] ligands, (ii) the effect of residence time on the desorption of AsO_4 by these ligands and (iii) the kinetics of AsO_4 desorption by PO_4. We studied with special attention the sorption/desorption of AsO_4 in the presence of PO_4, because PO_4 is an analogous of AsO_4 and shows a good capacity to compete with AsO_4 on both LDHs and Al and Fe-oxides [25]. Furthermore, competition in sorption of these anions on LDHs, which are present in soil environments (e.g., green rusts) [8,16,28] have received scant attention.

2. Materials and methods

2.1. Synthesis of Al–Mg and Fe–Mg layered double hydroxides

The LDHs of Mg-Al (Al–Mg-LDH) and Mg-Fe (Fe–Mg-LDH) were prepared by the coprecipitation method [9], whereby solutions containing $MgCl_2 \cdot 6H_2O$ and $AlCl_3 \cdot 6H_2O$ or $FeCl_3 \cdot 6H_2O$ (initial Mg/Al or Mg/Fe molar ratio equal to 2) were slowly added with stirring at 20 °C to NaOH solutions at pH 10.0. The suspension's pH was maintained for 24 h by adding $2 \, mol \, L^{-1}$ NaOH using an automatic titrator (Potentiograph E536 Metrom Herisau) in conjunction with an automatic syringe (burette 655 Dosimat), at 20 °C, after which they were centrifuged at $10,000 \times g$ for 30 min, rinsed five times with deionized water and then dialyzed for 21 days, freeze dried and lightly ground to pass through a 0.315 mm sieve. The Al–Mg-LDH and Fe–Mg-LDH precipitates obtained were used for the sorption/desorption studies. Note, no effort was made to minimize contact with the atmospheric air during the preparation of the LDHs, in order to simplify the preparation method. Sub-samples of the Fe–Mg-LDH and Al–Mg-LDH were aged for 30 days at 50 °C, in order to study the influence of aging on the degree of crystallinity of these materials.

2.2. Characterization of the LDHs

The Al–Mg-LDH and Fe–Mg-LDH precipitates were characterized by X-ray diffraction (XRD) and Fourier Transform Infrared (FT-IR) spectroscopy. The X-ray diffraction patterns of randomly oriented samples were obtained using a Rigaku diffractometer (Rigaku Co, Tokyo) equipped with Cu Kα radiation generated at 40 kV and 30 mA and a scan speed of $2° \, 2\theta \, min^{-1}$. The XRD traces were the results of eight summed signals. The FT-IR spectra of the LDH precipitates were obtained using diffuse reflectance infrared Fourier transform (DRIFT) spectroscopy. Sample preparation for the DRIFT determinations was as follows: 0.2 mg of the LDHs were mixed with 200 mg of over-dried KBr. The DRIFT spectra were obtained using a Perkin-Elmer Spectrum One FT-IR Spectrophotometer (Perkin Elmer USA), with a spectral resolution of $1 \, cm^{-1}$.

The surface area of the precipitates was determined by H_2O sorption at 20% relative humidity [29].

2.3. AsO_4 and PO_4 sorption isotherms

Suitable volumes of $0.1 \, mol \, L^{-1}$ solutions containing Na_2HAsO_4 or KH_2PO_4 were added to 100 mg of the LDHs, in order to have initial AsO_4 or PO_4 concentrations in the range of 4×10^{-4} to $1 \times 10^{-2} \, mol \, L^{-1}$ for the Al–Mg-LDH and in the range of 6×10^{-4} to $1.6 \times 10^{-2} \, mol \, L^{-1}$ for the Fe–Mg-LDH. The final volume was adjusted to 20 mL with $0.01 \, mol \, L^{-1}$ KCl and the initial LDH/solution ratio was $5 \, g \, L^{-1}$. The pH of each suspension was kept constant at 6.0 for 24 h at 20 °C by adding 0.1 or $0.01 \, mol \, L^{-1}$ HCl or KOH with the automatic titrator/syringe.

The sorption of AsO_4 onto the LDHs was carried out as a function of pH (4.0–10.0) by adding a suitable amount of AsO_4 (2100 and $3600 \, mmol \, kg^{-1}$ for Al–Mg-LDH and Fe–Mg-LDH, respectively, a quantity 40% higher than that necessary to reach a maximum sorption at pH 6.0, as determined from the sorption isotherms) to 100 mg of the LDHs. The pH of the systems was kept constant for 24 h at 20 °C by adding 0.1 or $0.01 \, mol \, L^{-1}$ HCl or KOH using the automatic titrator/syringe.

In a separate experiment, 20, 50, 100 or 200 mg of Al–Mg-LDH or Fe–Mg-LDH were added to 20 mL of a solution containing $1.33 \times 10^{-3} \, mol \, AsO_4 \, L^{-1}$ ($100 \, mg \, As \, L^{-1}$). The initial LDH/solution ratio ranged from 1 to $10 \, g \, L^{-1}$. The pH of each suspension was kept constant at 6.0 for 24 h at 20 °C by adding 0.1 or $0.01 \, mol \, L^{-1}$ HCl or KOH with the automatic titrator/syringe.

The suspensions were centrifuged at $10,000 \times g$ for 20 min and then filtered through a 0.22-μm membrane filter. The filtrates were stored at 2 °C until analysis. The experiments were conducted in triplicate.

2.4. Sorption of AsO_4 in the presence of inorganic and organic ligands

To 100 mg of the Fe–Mg-LDH or Al–Mg-LDH at pH 6.0 was added suitable amounts of a $0.1 \, mol \, L^{-1}$ Na_2HAsO_4 solution so that the AsO_4 surface coverage of the Fe–Mg-LDH ($2000 \, mmol \, kg^{-1}$) and Al–Mg-LDH ($600 \, mmol \, kg^{-1}$) was about 70%, based on the sorption isotherms and inorganic (NO_3 as $NaNO_3$, NO_2 as $NaNO_2$, PO_4 as KH_2PO_4, SeO_3 as $Na_2SeO_3 \cdot 5H_2O$, SO_4 as $MgSO_4 \cdot 7H_2O$) and organic (OX as $Na_2C_2O_4$, TAR as $C_4H_4Na_2O_6 \cdot 2H_2O$) ligands at initial ligand/AsO_4 molar ratio (R) of 1, 3 and 5. In the absence of competing ligands, all the AsO_4 added was completely sorbed after 24 h. The pH of each suspension was kept constant for 24 h at 20 °C by adding 0.1 or $0.01 \, mol \, L^{-1}$ HCl or KOH using the automatic titrator. The suspensions were then centrifuged at $10,000 \times g$ for 20 min and then filtered through a 0.22-μm membrane filter. The filtrates were stored at 2 °C until analysis. The experiment was conducted in triplicate.

2.5. Effect of residence time on the desorption of AsO_4 by inorganic and organic ligands

To 100 mg of the Fe–Mg-LDH or Al–Mg-LDH at pH 6.0 was added suitable amounts of a $0.1 \, mol \, L^{-1}$ Na_2HAsO_4 solution so that surface coverage of the Fe–Mg-LDH ($2000 \, mmol \, kg^{-1}$) and Al–Mg-LDH ($600 \, mmol \, kg^{-1}$) was about 70%, based on the sorption isotherms. The systems were maintained at pH 6.0 for 24, 48 or 168 h at 20 °C by adding 0.1 or $0.01 \, mol \, L^{-1}$ HCl or KOH using the automatic titrator. All the AsO_4 added was completely sorbed in the 24, 48 and 168 h systems. Inorganic (NO_3, NO_2, PO_4, SeO_3, SO_4) and organic (OX, TAR) ligands (initial ligand/AsO_4 molar ratio = 3) were then added to the 24, 48 or 168 h AsO_4 sorbed LDH systems. The final volume was 20 mL and the final LDH/solution ratio was $5 \, g \, L^{-1}$. After maintaining the systems at pH 6.0 with 0.1 or $0.01 \, mol \, L^{-1}$ HCl or KOH for 24 h at 20 °C with the automatic titrator, the suspensions were then centrifuged at $10,000 \times g$ for 20 min and then filtered through

a 0.22-μm membrane filter. The filtrates were stored at 2 °C until analysis. The experiment was conducted in triplicate.

2.6. Kinetics of desorption of AsO_4 by PO_4

The kinetic study was carried out using the 24 h AsO_4 sorbed Fe–Mg-LDH (2000 mmol kg^{-1}) and Al–Mg-LDH (600 mmol kg^{-1}) systems as described above and with an initial PO_4/AsO_4 molar ratio = 3. The amount of AsO_4 desorbed from the systems, maintained at pH 6.0 with 0.1 or 0.01 mol L^{-1} HCl or KOH (over the entire reaction period using the automatic titrator), by PO_4 was determined from 0.08 to 50 h at 20 °C. The suspensions from each sampling period were centrifuged at 10,000 × g for 20 min and then filtered through a 0.22-μm membrane filter. The filtrates were stored at 2 °C until analysis. The experiment was conducted in triplicate.

2.7. AsO_4 and PO_4 determination

AsO_4 and PO_4 in the filtrates were determined by ion chromatography [22,30], using a Dionex DX-300 Ion Chromatograph (Dionex Co, Sunnyvale, CA), an Ion Pac AS11 column (4.0 mm), an eluent of 0.02 mol L^{-1} NaOH at a flow rate of 1 mL min^{-1} and a CD 20 conductivity detector combined with autosuppression. The average AsO_4 and PO_4 retention times were 2.8 and 2.0 min, respectively. The standard AsO_4 and PO_4 concentrations used were 5×10^{-5} to 2×10^{-3} mol L^{-1} and 1×10^{-4} to 2×10^{-3} mol L^{-1}, respectively.

In the experiment where a 1.33×10^{-3} mol AsO_4 L^{-1} solution was kept to react in the presence of varying amounts of LDHs, AsO_4 concentration in the final solution was determined by an Hydride Generation Atomic Absorption Spectrophotometer (HG-AAS, AAnalyst 700, Perkin Elmer Instruments). The AsO_4 detection limit of this method was 2.7×10^{-8} mol L^{-1}.

The amount of AsO_4 or PO_4 sorbed was determined by the difference between the amount initially added and that determined in the filtrates. The data are the mean of three determinations. The ± values in Tables 2 and 3 indicate the standard deviation. The intraday repeatability study was carried out by the injection of the same standard solution five consecutive times ($n = 5$) in the same day under the same conditions. The interday precision was carried out for three successive days using the same conditions. The relative standard deviation of these measurements ranged from 1.8 to 3.2%.

3. Results and discussion

3.1. Nature of the LDHs

The X-ray diffraction patterns of the Al–Mg-LDH and Fe–Mg-LDH are shown in Fig. 1. Both LDHs showed peaks at about 0.760 (d_{003}), 0.380, 0.260, 0.153 and 0.150 nm and some asymmetric peaks at high angles (>30° 2θ), characteristic of hydrotalcite [1,7,9,10,31]. The peaks were sharp for the Al–Mg-LDH, whereas the peaks were broader for the Fe–Mg-LDH, which indicated that the Fe–Mg-LDH was less crystalline than the Al–Mg-LDH and/or the particles were of smaller size. However, prolonging the aging for 30 days at 50 °C a higher degree of crystallinity and/or larger particles size of Fe–Mg-LDH was obtained (Fig. 1), whereas Al–Mg-LDH remained practically unchanged (not shown). Probably, Fe–Mg-LDH sample aged 24 h at 20 °C was a mixture of materials of different crystallinities, size and nature (LDH and short-range ordered Fe and/or Mg oxides) [32]. The peaks from the Fe–Mg-LDH were also shifted 0.02 nm (0.2 Å) higher compared to the Al–Mg-LDH.

The FT-IR spectra of the Al–Mg-LDH and Fe–Mg-LDH are shown in Fig. 2. The Al–Mg-LDH spectrum showed a peak in the hydroxyl
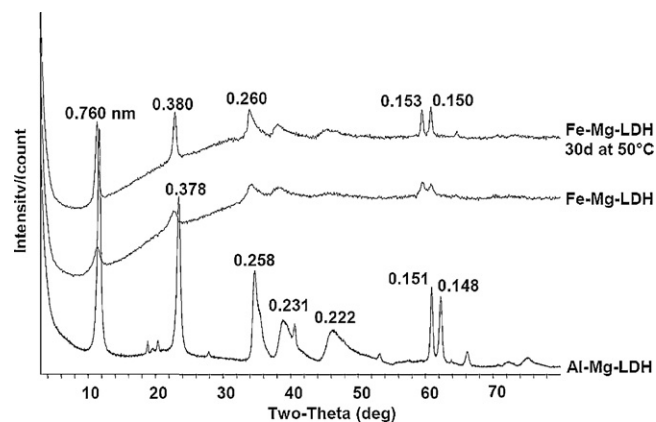
Fig. 1. Powder X-ray diffraction patterns of Al–Mg-LDH and Fe–Mg-LDH aged at 20 °C and Fe–Mg-LDH aged for 30 days at 50 °C.

stretching region centered at about 3450 cm^{-1}, attributed to the stretching vibrations of the hydroxyls attached to Al and Mg sheets and to water molecules in the basal interlayer [26]. The shoulder at about 3070 cm^{-1} was due to the interaction between the OH groups and the interlayer carbonate ions and the presence of the carbonate peak at 680 cm^{-1} also indicated that considerable amounts of carbonate were in the interlayer [26,31,33]. The peaks at about 940, 780, 550, 450 cm^{-1} were ascribed to the Al-O stretching modes (Fig. 2A). The strong peak at 1356 cm^{-1} is due to carbonate mainly present in the basal interlayer. In a Zn-Al-Cl-LDH
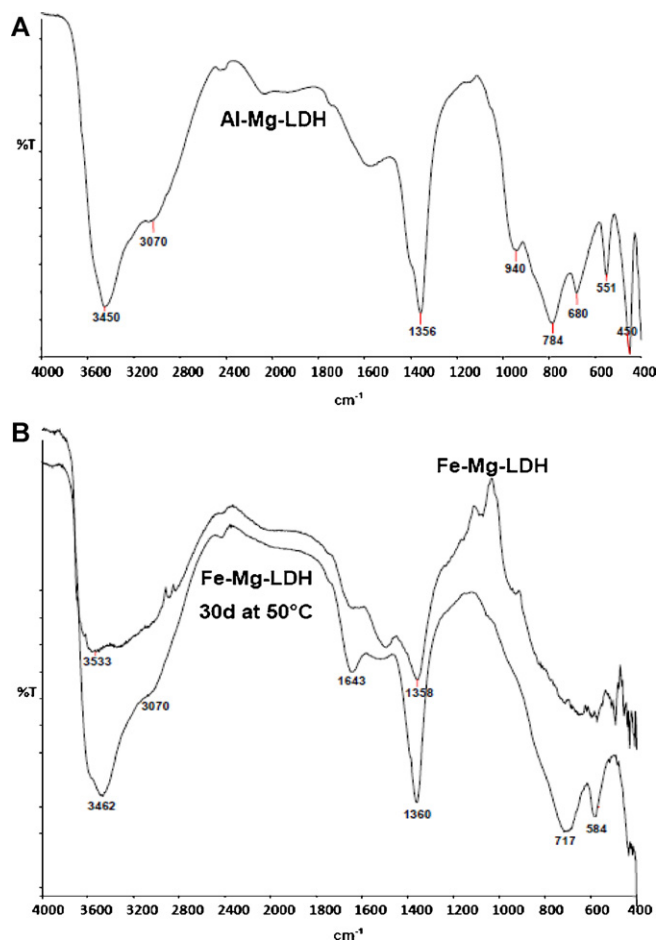
Fig. 2. FR-IR spectra of Al–Mg-LDH (A) and Fe–Mg-LDH aged at 20 °C (B) and Fe–Mg-LDH aged for 30 days at 50 °C (B).
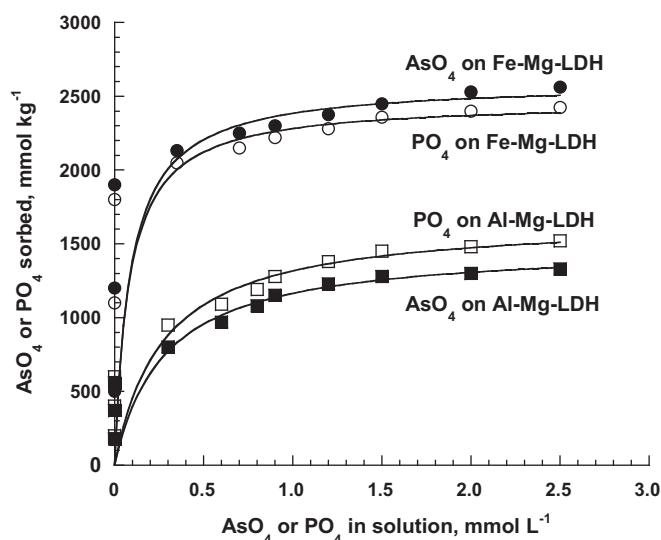
Fig. 3. Sorption isotherms of AsO_4 and PO_4 onto Al–Mg-LDH and Fe–Mg-LDH at 20 °C and pH 6.0, after a reaction period of 24 h.

Fig. 4. Effect of pH on the sorption of AsO_4 at 20 °C onto Al–Mg-LDH and Fe–Mg-LDH after a reaction period of 24 h.

prepared in boil and N_2 purged water, a very weak carbonate peak (1354 cm^{-1}) was observed in the IR spectrum [34]. The ratio of the hydroxyl/carbonate peak was 6, compared to 1 in this study, indicating that the carbonate concentration in the basal interlayers in this study was significant. The spectrum of Fe–Mg-LDH also had a strong carbonate peak at 1358 cm^{-1} indicating that significant amounts of carbonate were in the basal interlayer (Fig. 2B). The hydroxyl stretching region and the metal bands below 1000 cm^{-1} in the Fe–Mg-LDH aged 24 h at 20 °C appeared particularly broad indicating a lower crystallinity and/or smaller size of the particles [26], which is in agreement with the XRD results.

3.2. Sorption of AsO_4

The sorption isotherms of AsO_4 onto the Al–Mg-LDH and Fe–Mg-LDH at pH 6.0, after 24 h of reaction, are shown in Fig. 3. The sorption data of AsO_4 sorbed onto the LDH conformed to the Langmuir equation in the following form:

$$S = \frac{S_m Kc}{1 + Kc}$$

where S is the amount of AsO_4 sorbed per unit mass of adsorbent (mmol kg^{-1}), S_m is the maximum amount of AsO_4 that may be bound to the adsorbent (sorption capacity), c is the equilibrium solution concentration (mmol L^{-1}), and K is a constant related to the binding energy [35].

The sorption isotherms of AsO_4 to the two LDHs were typical L shaped curves [35], indicating that AsO_4 had a high affinity for the sorption sites on the LDHs, exchanging with the Cl and CO_3 ions in the interlayer. The Fe–Mg-LDH sorbed nearly twice the amount (mmol kg^{-1}) of AsO_4 compared to the Al–Mg-LDH (Fig. 3), due, in part, to its greater surface area (273 and 219 m^2 g^{-1}, respectively) and lower degree of crystallinity. The sorption isotherms of PO_4, which is an analogous of AsO_4 and showed a strong
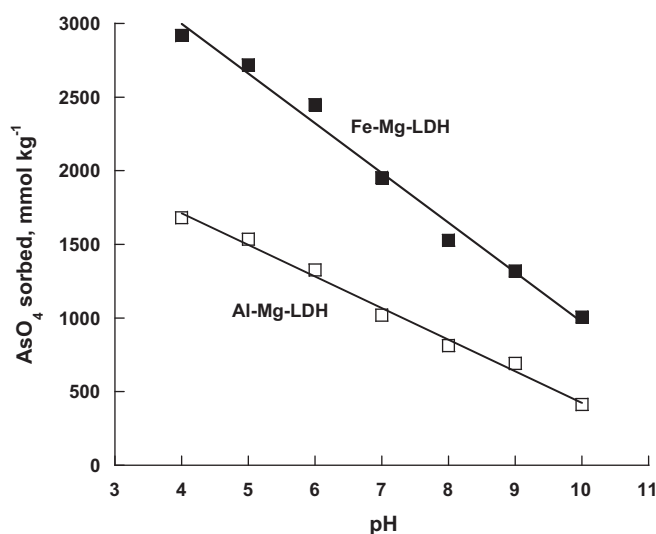
capacity to compete with AsO_4 (as discussed below) was also studied. The Fe–Mg-LDH sorbed more AsO_4 (S_m = 2595 mmol kg^{-1}) than PO_4 (S_m = 2470 mmol kg^{-1}), in contrast to the Al–Mg-LDH, which adsorbed more PO_4 (S_m = 1675 mmol kg^{-1}) than AsO_4 (S_m = 1490 mmol kg^{-1}) (Table 1). These findings would be attributed to the greater affinity of AsO_4 than PO_4 for Fe sites and, vice versa, to the greater affinity of PO_4 than AsO_4 for Al sites [25]. Violante et al. [25] also observed the same trend for AsO_4 and PO_4 sorbed on Fe-rich and Al-rich minerals.

The Langmuir constant K was around an order of magnitude larger for the Fe–Mg-LDH compared to the Al–Mg-LDH for both AsO_4 and PO_4 (Table 1), indicating a higher affinity of the Fe–Mg-LDH for the anions, probably due to the presence of short-range Fe and/or Mg precipitates in this sample on which both AsO_4 and PO_4 may form strong inner-sphere complexes [28].

The effect of pH (from 4.0 to 10.0) on the sorption of AsO_4 onto Al–Mg-LDH and Fe–Mg-LDH samples, after 24 h of reaction, is shown in Fig. 4. AsO_4 sorption onto the samples decreased by increasing pH. The rate of decline in the amount of AsO_4 sorbed was, however, relatively constant, decreasing the fastest for the Fe–Mg-LDH (270 mmol AsO_4/pH unit) compared to the Al–Mg-LDH (210 mmol AsO_4/pH unit). This behavior would be attributed to the high affinity of OH ions for LDHs [1,22] and/or to the value of zero point charge (pzc) of two sorbents. At pH < pzc, the positively charged surfaces of the sorbents facilitated the sorption of the negatively charged AsO_4. The pzc for LDHs was reported to be in the range 7.0–9.0 [26], so in alkaline systems the sorption of AsO_4 anions onto the LDH surfaces would be inhibited. At pH > pzc, OH ions dominate the system, resulting in a charge reversal on the surfaces of the sorbents which led to electrostatic repulsion of AsO_4 ions.

In the experiment carried out adding increasing amounts of the LDHs (1, 2.5, 5 or 10 g) to 1 L of solution containing 1.33×10^{-3} mol AsO_4 L^{-1} (100 mg As L^{-1}), we found that 1 g of

Table 1
Langmuir sorption capacity (S_m) and the constant K for AsO_4 and PO_4 as obtained from the sorption isotherms of the LDH.

Sample	Surface area (m^2 g^{-1})	AsO_4			PO_4		
		S_m (mmol kg^{-1})	K	R^2	S_m (mmol kg^{-1})	K	R^2
Al–Mg-LDH	219	1490 (6.8)[a]	3.3	0.98	1675 (7.6)[a]	3.9	0.95
Fe–Mg-LDH	273	2595 (9.5)[a]	31.0	0.94	2470 (9.0)[a]	20.6	0.96

[a] Numbers in parenthesis indicate the amount sorbed as mmol m^{-2} × 10^{-3}.

Table 2
Effect of residence time on AsO_4 desorption (%) from the Al–Mg-LDH by inorganic and organic ligands after a reaction time of 24 h.

Ligand	Residence time, h	AsO_4 sorbed[a], mmol kg^{-1}	AsO_4 desorbed, %
NO$_3$	24	588.6 ± 11.0	1.9 ± 0.2
	48	590.1 ± 8.6	1.6 ± 0.1
	168	594.8 ± 4.7	0.9 ± 0.1
NO$_2$	24	557.3 ± 28.1	7.1 ± 0.5
	48	563.4 ± 37.2	6.1 ± 0.6
	168	581.2 ± 17.6	3.1 ± 0.3
SeO$_3$	24	539.6 ± 44.3	10.1 ± 0.5
	48	545.2 ± 37.6	9.1 ± 0.6
	168	568.3 ± 28.7	5.3 ± 0.7
SO$_4$	24	524.8 ± 30.8	12.5 ± 1.0
	48	533.4 ± 33.5	11.1 ± 0.7
	168	562.4 ± 28.9	6.3 ± 0.5
TAR	24	486.4 ± 42.1	18.9 ± 1.8
	48	493.4 ± 37.5	17.8 ± 1.5
	168	503.5 ± 28.6	16.1 ± 1.1
OX	24	414.0 ± 22.3	31.0 ± 1.7
	48	432.7 ± 36.7	27.9 ± 1.8
	168	475.9 ± 30.5	20.7 ± 1.6
PO$_4$	24	163.2 ± 15.4	72.8 ± 5.5
	48	184.6 ± 16.5	69.2 ± 3.8
	168	224.1 ± 18.1	62.6 ± 2.9

[a] AsO_4 added initially was 600 mmol kg^{-1}, initial ligand/AsO_4 molar ratio = 3.

the Al–Mg-LDH or Fe–Mg-LDH dropped the concentration of AsO_4 to 1.28×10^{-6} mol L^{-1} (0.096 mg As L^{-1}) and 1.24×10^{-6} mol L^{-1} (0.093 mg As L^{-1}), respectively, whereas the addition of 10 g of the Al–Mg-LDH or Fe–Mg-LDH dropped the concentration of the above mentioned solution to 3.06×10^{-7} mol L^{-1} (0.023 mg As L^{-1}) and 2.26×10^{-7} mol L^{-1} (0.017 mg As L^{-1}), respectively (data not shown). By interpolation of these data with an exponential curve, we found that the addition of 15.3 and 13.0 g L^{-1} of Al–Mg-LDH and Fe–Mg-LDH, respectively, would be enough to drop the concentration of the 1.33×10^{-3} mol AsO_4 L^{-1} (100 mg As L^{-1}) solution to the world health organization limit, equal to 1.33×10^{-7} mol AsO_4 L^{-1} (0.01 mg As L^{-1}).

3.3. Sorption of AsO_4 in the presence of inorganic and organic ligands

The sorption of AsO_4 in the presence of increasing concentrations of inorganic (NO$_3$, NO$_2$, PO$_4$, SeO$_3$, SO$_4$) and organic (OX, TAR) ligands on Al–Mg-LDH and Fe–Mg-LDH, at pH 6.0, after 24 h of reaction, are shown in Fig. 5. The initial ligand/AsO_4 molar ratio (R) was 1, 3 and 5, but only the data at R = 1 and 5 are shown for sake of clarity. The efficiency (%) of the ligands in preventing AsO_4 sorption is calculated by subtracting the amount sorbed from that initially added, divided by the amount initially added. The efficiency of the anions to compete with AsO_4 for the sorption sites on the Al–Mg-LDH was in the order NO$_3$ < NO$_2$ < SO$_4$ < SeO$_3$ < TAR < OX ≪ PO$_4$ at all molar ratios examined (Fig. 5A), while on the Fe–Mg-LDH the order was NO$_3$ < SO$_4$ ≈ NO$_2$ < TAR < OX < SeO$_3$ ≪ PO$_4$ (Fig. 5B).

The inhibition of AsO_4 sorption increased by increasing the initial ligand concentration and was greater on Al–Mg-LDH than on Fe–Mg-LDH, evidently because AsO_4 anions have a stronger affinity for Fe than Al [25] and for the presence in Fe–Mg-LDH of short-range-ordered materials on which AsO_4 forms very strong inner-sphere complexes not easily desorbable by competing ligands [18,36].

Many factors affect the sorption of organic and inorganic anions onto LDHs as the valency, the size and the capacity of each single ligand to form outer- or inner-sphere complexes on the surfaces of the minerals. The negligible effect of NO$_3$ and NO$_2$ on AsO_4 sorption could be ascribed to the fact that these ions are monovalent and are nonspecific anions in solid–liquid interfacial reactions [23]. Furthermore, they have a lower ionic potential than AsO_4, resulting

in their weaker competition ability with AsO_4 for binding sites on LDHs [23].

SO_4 is expected to form outer-sphere complexes on clay surfaces [8,22,30] at pH ≥6, while SeO$_3$, OX, TAR and PO$_4$ are all expected to form inner-sphere complexes, which probably accounts for the low competitiveness of SO_4 compared to the other anions with AsO_4 for the sorption sites on the LDH surfaces.

The only difference in the order between the two LDHs being that the organic acids were less effective than SeO$_3$ in competing with AsO_4 on the Fe–Mg-LDH versus the Al–Mg-LDH. The efficiency of SeO$_3$ to inhibit AsO_4 sorption was lightly greater on Fe–Mg-LDH than Al–Mg-LDH; in fact, SeO$_3$ replaced more AsO_4 from Fe–Mg-LDH than Al–Mg-LDH (as discussed below).

The 10–20% decrease in efficiency of the organics for the Fe–Mg-LDH compared to the Al–Mg-LDH systems indicated that the affinity of the organic acids for the sorption sites on the two LDH was different, attributed to the difference in their bonding with the Al and Fe in the LDHs. The results are contrary to that expected based on the stability constants (log$k$) for tartrate-Fe (6.5), oxalate-Fe (7.6), tartrate-Al (5.84) and oxalate-Al (6.28) [37].
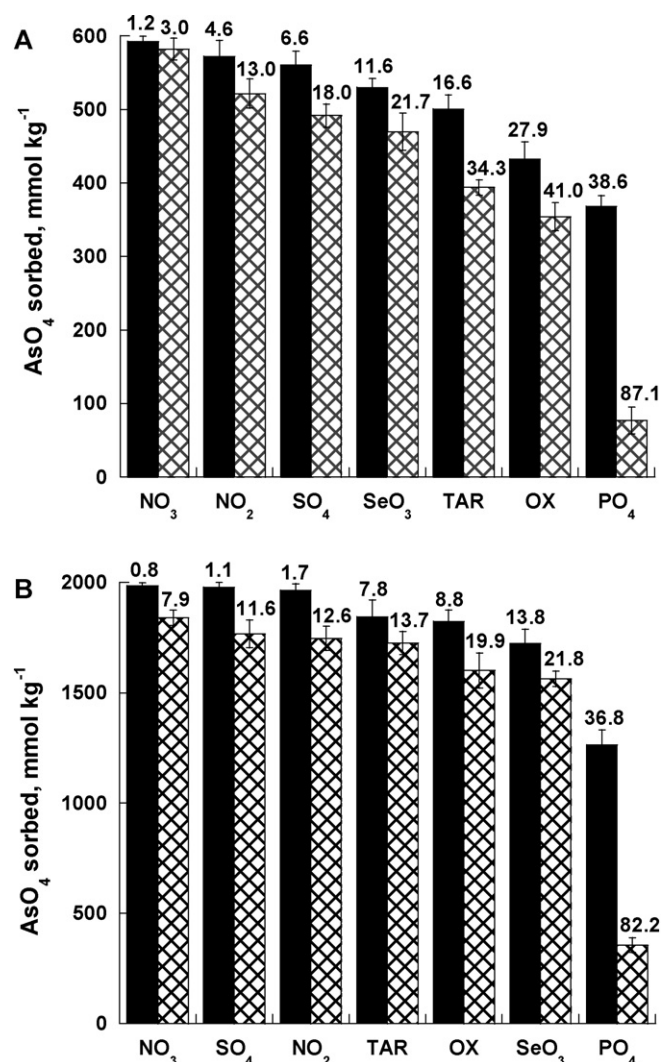

Fig. 5. The amount of AsO_4 sorbed onto the Al–Mg-LDH (A) and Fe–Mg-LDH (B) in the presence of increasing concentrations of inorganic and organic ligands after a reaction time of 24 h; initial ligand/AsO_4 molar ratio = 1 (black) and 5 (checkered white). The numbers indicate the efficiency (%) of the ligands in preventing AsO_4 sorption. The initial AsO_4 concentration for the Al–Mg-LDH and Fe–Mg-LDH was 600 and 2000 mmol kg^{-1}, respectively.

Table 3
Effect of residence time on AsO_4 desorption (%) from the Fe–Mg-LDH by inorganic and organic ligands after a reaction time of 24 h.

Ligand	Residence time, h	AsO_4 sorbed[a], mmol kg^{-1}	AsO_4 desorbed, %
NO_3	24	1929.4 ± 58.0	3.5 ± 0.2
	48	1952.2 ± 40.6	2.4 ± 0.2
	168	1990.1 ± 8.8	0.5 ± 0.1
SO_4	24	1920.4 ± 66.1	4.0 ± 0.3
	48	1939.7 ± 52.8	3.0 ± 0.2
	168	1986.5 ± 12.2	0.7 ± 0.1
NO_2	24	1911.3 ± 71.8	4.4 ± 0.3
	48	1942.1 ± 49.1	2.9 ± 0.2
	168	1980.2 ± 15.4	1.0 ± 0.1
TAR	24	1804.9 ± 112.2	9.8 ± 0.5
	48	1826.9 ± 77.5	8.7 ± 0.6
	168	1860.1 ± 88.4	7.0 ± 0.6
OX	24	1791.1 ± 100.6	10.4 ± 0.5
	48	1856.6 ± 89.7	7.2 ± 0.4
	168	1969.7 ± 24.8	1.5 ± 0.1
SeO_3	24	1703.7 ± 90.2	14.8 ± 1.2
	48	1784.3 ± 82.3	10.8 ± 0.6
	168	1891.8 ± 78.8	5.4 ± 0.4
PO_4	24	749.5 ± 42.6	62.5 ± 4.9
	48	810.5 ± 60.2	59.5 ± 4.7
	168	910.8 ± 57.8	54.5 ± 5.1

[a] AsO_4 added initially was 2000 mmol kg^{-1}, initial ligand/AsO_4 molar ratio = 3.

Divalent forms of OX and TAR are expected to exist in solution at pH 6.0 (pKa values for OX = 1.2, 4.2; TAR = 2.98, 4.34; SeO_3 = 2.46, 7.3), which could account for them competing more effectively with AsO_4 than SeO_3 on the Al–Mg-LDH but does not explain why SeO_3 competed more effectively with AsO_4 than the organic acids for the sorption sites on the Fe–Mg-LDH. A possible explanation of this behavior is that SeO_3 seems to form a mixture of outer-sphere and inner-sphere complexes on minerals containing Al, whereas forms inner-sphere complexes on goethite and ferrihydrite [38]. Furthermore, anion size and anion orientation were observed to influence sorption of anions in the interlayer of LDHs [39]. Thus, differences in the steric and electronic factors of the sorption sites in the interlayer of the Al–Mg-LDH and Fe–Mg-LDH and/or of the anions likely influenced the affinity of the organic acids for the sorption sites.

3.4. Effect of residence time on the desorption of arsenate

Initially AsO_4 was sorbed by the Al–Mg-LDH (600 mmol kg^{-1}) and Fe–Mg-LDH (2000 mmol kg^{-1}) at pH 6.0 for either a reaction period of 24, 48 or 168 h (i.e., residence time). The desorption of AsO_4 from the Al–Mg-LDH and Fe–Mg-LDH by the inorganic and organic ligands, for an initial ligand/AsO_4 molar ratio (R) of 3, as affected by the residence time of AsO_4 are shown in Tables 2 and 3, respectively. The amounts of AsO_4 desorbed from the LDHs decreased with an increase in the AsO_4 residence time. Precisely, the quantities of AsO_4 removed by PO_4 decreased from 72.8 to 62.6% from Al–Mg-LDH (Table 2) and from 62.5 to 54.5% from Fe–Mg-LDH (Table 3) by increasing the residence time of AsO_4 from 24 to 168 h.

After a residence time of 168 h the amounts of AsO_4 replaced by OX, TAR, SeO_3, SO_4, NO_2 and NO_3 from Al–Mg-LDH ranged from 20.7% by OX to 0.9% by NO_3. The capacity of these ligands in removing AsO_4 from Fe–Mg-LDH was still lower ranging from 7.0% for TAR to 0.7% for NO_3, evidencing that AsO_4 is more strongly sorbed on minerals containing Fe than Al. Negligible amounts of AsO_4 (<5%) were replaced by NO_2 and NO_3.

Other studies on Fe and Al oxides [22,40] have also shown that an increase in residence time of AsO_4 resulted in a decrease in its desorption by competing anions. Clearly, increased diffusion into the LDH and the formation of a stronger bond between the AsO_4 and the surface sorption sites of the sorbents may account for reduce efficiency with an increase in the AsO_4 residence time.

The ability of the anions to desorb AsO_4 from the sorption sites on the Al–Mg-LDH was in the order $NO_3 < NO_2 < SeO_3 \approx SO_4 < TAR < OX \ll PO_4$ at all residence times examined (Table 2), while on the Fe–Mg-LDH the order was $NO_3 < SO_4 \approx NO_2 < TAR \leq OX < SeO_3 \ll PO_4$ (Table 3).

The effect of increasing residence time on desorbing AsO_4 was similar for all the ligands, for both LDHs, varying from 2 to 10%. However, for the Al–Mg-LDH systems with PO_4, TAR and OX, 10–20% more AsO_4 was desorbed compared to the Fe–Mg-LDH systems for the same residence time, due to the fact that AsO_4 was more strongly sorbed by the Fe–Mg-LDH than the Al–Mg-LDH [28].

Comparison of these trends to that observed for the systems where both ligand and AsO_4 were added simultaneously (Fig. 5) showed that they were the same, but under the same conditions lower amounts of AsO_4 were replaced by all the ligands when AsO_4 was sorbed before ligands.

3.5. Kinetics of AsO_4 desorption by PO_4

The amount of AsO_4 initially sorbed by the Al–Mg-LDH and Fe–Mg-LDH was 600 and 2000 mmol kg^{-1}. The AsO_4 desorbed from
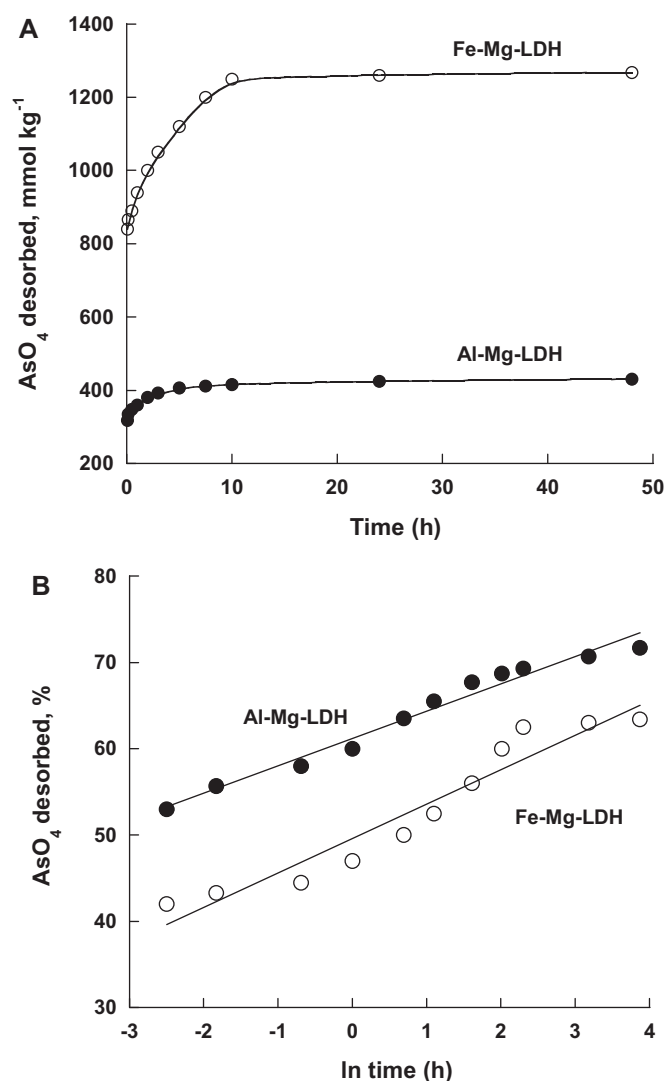

Fig. 6. Kinetics of desorption of AsO_4 by PO_4 from the Al–Mg-LDH and Fe–Mg-LDH (A), also described by the Elovich equation (B). The initial AsO_4 concentration for the Al–Mg-LDH and Fe–Mg-LDH was 600 and 2000 mmol kg^{-1}, respectively. The initial PO_4/AsO_4 molar ratio was 3.

Table 4
Kinetic parameters by simply regression analysis of AsO_4 desorption by PO_4 for the reaction period 5 min to 48 h for the LDH using the Elovich kinetic equation.

Sample	Elovich kinetic equation	R^2	$P(\times 10^{-8})$	F	$\alpha^b(\times 10^5)$	β^b
Al–Mg-LDH	$q_t^a = 288.9 + 19.03 \ln(t)$	0.971	1.81	342	745	0.0525
Fe–Mg-LDH	$q_t = 662.6 + 80.1 \ln(t)$	0.921	175	119	3.13	0.0124

[a] q_t is the amount of AsO_4 desorbed (mmol kg^{-1}) in time t (min).
[b] α and β are Elovich coefficient obtained from the Elovich kinetic model $q_t = (1/\beta)\ln(\alpha\beta) + (1/\beta)\ln(t)$.

the LDHs by PO_4 (initial PO_4/AsO_4 molar ratio of 3), as a function of time, was shown in Fig. 6. The amounts of AsO_4 desorbed from the LDHs increased with time, being characterized by an initially very fast desorption reaction followed by a much slower desorption reaction until a plateau was reached (Fig. 6A). The amount of AsO_4 desorbed at 5 min for the Al–Mg-LDH and Fe–Mg-LDH was 53 and 42%, respectively, indicating that some AsO_4 was slightly more strongly bound to the Fe–Mg-LDH versus the Al–Mg-LDH. After a reaction period of 24 h the Al–Mg-LDH and Fe–Mg-LDH released 70 and 63% of the bound AsO_4, respectively, suggesting that the main difference between the two LDHs was in the amount of more easily desorbable AsO_4, that is, less strongly bound AsO_4. In contrast, for Al and Fe (oxy)hydroxides about 25 and 15% of the AsO_4 was desorbed by PO_4 (initial PO_4/AsO_4 $R = 4$) after a reaction period of 24 h [22]. Hence, AsO_4 was more strongly sorbed by the Al and Fe (oxy)hydroxides versus the LDHs.

The kinetics of AsO_4 desorption were well described by the Elovich equation (Fig. 6B). The linear form of this equation [22] is given by

$$q_t = \frac{1}{\beta} \ln(\alpha\beta) + \frac{1}{\beta} \ln(t)$$

where q_t is the amount of AsO_4 desorbed for a given time (t), and α and β are the Elovich coefficients, representing the initial desorption rate (mmol kg^{-1} min^{-1}) and the desorption coefficient (mmol kg^{-1}), respectively.

The initial AsO_4 desorption rate coefficient (α) and desorption coefficient (β) were larger for the Al–Mg-LDH than the Fe–Mg-LDH (Table 4), which also supports the contention that the difference between the two LDHs was in the amount of easily desorbable AsO_4.

4. Conclusions

Differences in the steric and electronic factors of the sorption sites in the interlayer of the Al–Mg-LDH and Fe–Mg-LDH and/or of the anions influenced sorption/desorption of AsO_4. The sorption isotherms showed that the incorporation of Fe into Mg-LDH versus Al resulted in the sorption of more AsO_4. AsO_4 sorption on the LDHs varied with different competing anions, and the efficiency of the organic ligands in competing with AsO_4 differed between the two LDHs. The desorption of AsO_4 by the anions decreased with increasing AsO_4 residence time. The AsO_4/PO_4 desorption kinetics experiment indicated that there were greater amounts of more easily desorbable AsO_4 on the Al–Mg-LDH compared to the Fe–Mg-LDH.

The synthesis of LDHs of different chemical compositions and their ability to effectively sorb anions in the presence of competing anions deserves further attention.

Acknowledgment

References

[1] F. Cavani, F. Trifirb, A. Vaccari, Hydrotalcite-type anionic clays: preparation, properties and applications, Catal. Today 11 (1991) 173–301.
[2] S.P. Newman, W. Jones, Synthesis, characterization and applications of layered double hydroxides containing organic guests, New J. Chem. 22 (1998) 105–115.
[3] V. Rives, Layered Double Hydroxides: Present and Future, Nova Science Publishers Inc., New York, 2001.
[4] D.G. Evans, X. Duan, Preparation of layered double hydroxides and their applications as additives in polymers, as precursors to magnetic materials and in biology and medicine, Chem. Commun. (2006) 485–496.
[5] M.B.A. Rahman, M. Basri, M.Z. Hussein, M.N.H. Idris, R.N.Z.R.A. Rahman, A.B. Salleh, Immobilization of lipase from Candida rugosa on layered double hydroxides of Mg/Al and its nanocomposite as biocatalyst for the synthesis of ester, Catal. Today 93–95 (2004) 405–410.
[6] N.N. Das, J. Konar, M.K. Mohanta, S.C. Srivastava, Adsorption of Cr(VI) and Se(IV) from their aqueous solutions onto Zr^{4+}-substituted ZnAl/MgAl-layered double hydroxides: effect of Zr^{4+} substitution in the layer, J. Colloid Interface Sci. 270 (2004) 1–8.
[7] S. Miyata, The syntheses of hydrotalcite-like compounds and their structure and physico-chemical properties. The systems $Mg^{2+}–Al^{3+}–NO_3^-$, $Mg^{2+}–Al^{3+}–Cl^-$, $Mg^{2+}–Al^{3+}–ClO_4^-$, $Ni^{2+}–Al^{3+}–Cl^-$ and $Zn^{2+}–Al^{3+}–Cl^-$, Clays Clay Miner. 23 (1975) 369–375.
[8] A. Violante, G.S.R. Krishnamurti, M. Pigna, Mobility of trace elements in soil environments, in: A. Violante, P.M. Huang, G.M Gadd (Eds.), Biophysicochemical Processes of Metals and Metalloids in Soil Environments, John Wiley & Sons, Hoboken, NJ, 2008, pp. 169–213.
[9] V.R.L. Costantino, T.J. Pinnavaia, Basic properties of Mg^{2+}_{1-x} Al^{3+}_x layered double hydroxides intercalated by carbonate, hydroxide chloride and sulphate anions, Inorg. Chem. 34 (1995) 883–892.
[10] M.A. Ulibarri, I. Pavlovic, C. Barriga, M.C. Hermosin, J. Cornejo, Adsorption of anionic species on hydrotalcite-like compounds: effect of interlayer anion and crystallinity, Appl. Clay Sci. 18 (2001) 17–27.
[11] N.K. Lazaridis, A. Hourzemanoglou, K.A. Matis, Flotation of metal-loaded clay anion exchangers. Part II. The case of arsenates, Chemosphere 47 (2002) 319–324.
[12] M.M. Karim, Arsenic in groundwater and health problems in Bangladesh, J. Water Res. 34 (1999) 304–310.
[13] P.L. Smedley, D.G. Kinniburgh, A review of the source, behaviour and distribution of arsenic in natural waters, Appl. Geochem. 17 (2002) 517–568.
[14] W.T. Frankenberger Jr., Environmental Chemistry of Arsenic, Marcel Dekker, New York, 2002.
[15] A. Violante, S. Del Gaudio, M. Pigna, Adsorption–desorption processes of arsenate in soil environments, in: P.M. Huang, A. Violante, J.M. Bollag, P. Vityakon (Eds.), Soil Abiotic and Biotic Interactions and Impact on the Ecosystem and Human Welfare, Science Publishers, Enfield, NH, 2005, pp. 269–299.
[16] D. Mohan Jr., C.U. Pittman, Arsenic removal from water/wastewater using adsorbents. A critical review, J. Hazard. Mater. 142 (2007) 1–53.
[17] A. Violante, M. Ricciardella, S. Del Gaudio, M. Pigna, Coprecipitation of arsenate with metal oxides: nature, mineralogy and reactivity of aluminum precipitates, Environ. Sci. Technol. 40 (2006) 4961–4967.
[18] A. Violante, M. Pigna, S. Del Gaudio, M. Ricciardella, D. Banerjee, Coprecipitation of arsenate within metal oxides: nature, mineralogy and reactivity of iron(III) precipitates, Environ. Sci. Technol. 41 (2007) 8275–8280.
[19] L. Yang, Z. Shahrivari, P.K.T. Liu, M. Sahimi, T.T. Tsotsis, Removal of trace levels of arsenic and selenium from aqueous solutions by calcined and uncalcined layered double hydroxides (LDH), Ind. Eng. Chem. Res. 44 (2005) 6804–6815.
[20] L. Yang, M. Dadwhal, Z. Shahrivari, M. Ostwal, P.K.T. Liu, M. Sahimi, T.T. Tsotsis, Adsorption of arsenic on layered double hydroxides (LDH): effect of particle size, Ind. Eng. Chem. Res. 45 (2006) 4742–4751.
[21] G.P. Gillman, A simple technology for arsenic removal from drinking water using hydrotalcite, Sci. Total Environ. 366 (2006) 926–931.
[22] M. Pigna, G.S.R. Krishnamurti, A. Violante, Kinetics of arsenate sorption-desorption from metal oxides: effect of residence time, Soil Sci. Soc. Am. J. 70 (2006) 2017–2027.
[23] K.H. Goh, T.T. Lim, Influences of co-existing species on the sorption of toxic oxyanions from aqueous solution by nanocrystalline Mg/Al layered double hydroxide, J. Hazard. Mater. 180 (2010) 401–408.
[24] J. Zhu, M. Pigna, V. Cozzolino, A.G. Caporale, A. Violante, Sorption of arsenite and arsenate on ferrihydrite: effect of organic and inorganic ligands, J. Hazard. Mater. 189 (2011) 564–571.
[25] A. Violante, M. Pigna, Competitive sorption of arsenate and phosphate on different clay minerals and soils, Soil Sci. Soc. Am. J. 66 (2002) 1788–1796.
[26] A. Violante, M. Pucci, V. Cozzolino, J. Zhu, M. Pigna, Sorption/desorption of arsenate on/from Mg–Al layered double hydroxides: influence of phosphate, J. Colloid Interface Sci. 333 (2009) 63–70.
[27] Y.W. You, H.T. Zhao, G.F. Vance, Removal of arsenite from aqueous solutions by anionic clays, Environ. Technol. 22 (2001) 1447–1457.

[28] Y. Wang, G. Morin, G. Ona-Nguema, F. Juillot, F. Guyot, G. Calas, G.E. Brown Jr., Evidence for different surface speciation of arsenite and arsenate on green rust: an EXAFS and XANES study, Environ. Sci. Technol. 44 (2010) 109–115.

[29] J.P. Quirk, Significance of surface area calculated from water vapor sorption isotherms by use of the B.E.T. equation, Soil Sci. 80 (1955) 423–430.

[30] F. Liu, A. De Cristofaro, A. Violante, Effect of pH, phosphate and oxalate on the adsorption/desorption of arsenate on/from goethite, Soil Sci. 166 (2001) 197–208.

[31] V. Rives, Characterization of layered double hydroxides and their decomposition products, Mater. Chem. Phys. 75 (2002) 19–25.

[32] A. Violante, P.M. Huang, Formation mechanisms of aluminum hydroxide polymorphs, Clays Clay Miner. 41 (1993) 590–597.

[33] L. Lv, J. He, M. Wei, D.G. Evans, X. Duan, Uptake of chloride ion from aqueous solution by calcined layered double hydroxides: equilibrium and kinetic studies, Water Res. 40 (2006) 735–743.

[34] M. Islam, R. Patel, Synthesis and physicochemical characterization of Zn/Al chloride layered double hydroxide and evaluation of its nitrate removal efficiency, Desalination 256 (2010) 120–128.

[35] C.H. Giles, D. Smith, A. Huiston, A general treatment and classification of the solute adsorption isotherm. I. Theoretical, J. Colloid Interface Sci. 47 (1974) 755–765.

[36] S. Goldberg, C.T. Johnston, Mechanisms of arsenic adsorption on amorphous oxides evaluated using macroscopic measurements, vibrational spectroscopy, and surface complexation modeling, J. Colloid Interface Sci. 234 (2001) 204–216.

[37] A.E. Martell, R.M. Smith, Critical Stability Constants, Other Organic Ligands, vol. 3, Plenum Press, New York, 1977.

[38] D. Peak, Adsorption mechanisms of selenium oxyanions at the aluminum oxide/water interface, J. Colloid Interface Sci. 303 (2006) 337–345.

[39] M.M. Meyn, K. Beneke, G. Lagaly, Anion-exchange reactions of layered double hydroxides, Inorg. Chem. 29 (1990) 5201–5207.

[40] Y. Arai, D.L. Sparks, Residence time effects on arsenate surface speciation at the aluminum oxide–water interface, Soil Sci. 167 (2002) 303–314.